JOURNAL OF PROPULSION AND POWER
Vol. 23, No. 6, November–December 2007

Simulation of an Electrostatically Driven Microinjector

G. Krishnan,* J. W. Daily,† and J. Nabity‡
University of Colorado at Boulder, Boulder, Colorado 80309-0427

DOI: 10.2514/1.24334

This paper presents results of analytical and numerical simulations of an electrostatically actuated microfuel injector. The electrostatic-structural coupling, efficiency of valves, and net flow rate of the pump are calculated using analytical relations and compared with numerical simulations. One way to increase flow rate is to increase the stroke volume, which may lead to large deflection of the diaphragm. Thus, the membrane load deflection relationship is no longer linear and when coupled to the inherently nonlinear fluid behavior leads to a complex problem. We used numerical methods to solve for the fluid–structure interaction and the large deflection of the membrane, and studied the effect of actuation frequency on the net flow rate.

I. Introduction

OUR work is motivated by a desire to develop fuel injectors capable of working in a liquid-fueled pulsed detonation engine (PDE). The PDE operating environment imposes severe constraints on the fuel injection, atomization, evaporation, and mixing process. For example, Brophy et al. [1,2] showed that the droplet Sauter mean diameter should be less than 3 μm for successful deflagration-to-detonation transition (DDT) at cold start conditions. In addition, the injector must be able to operate at frequencies of up to 100 Hz with no-drip shutoff so as to avoid premature deflagration during the purge/fill cycle. Inkjet printing technologies have long demonstrated the capability to inject small droplets at high-repetition rates. We are therefore exploring the use of both micro- and mesoscale technology to form the basis of an appropriate injection technology. We have developed pump designs and the fabrication methodology to produce test units and have started testing first generation devices. The purpose of this work is to aid in optimizing the pump design for maximum performance and to understand the limitations of simple analytical models. In this paper, we thus explore the performance of the pump using both analytic and numerical analysis. The effect of large membrane deformations is also studied numerically.

Micropumps are devices that are used to pump, control, or manipulate small fluid volumes in systems. They are used in a wide array of applications, ranging from chemical and biological assay systems, to propulsion systems for space exploration. Thomas and Bessman [3] realized the first micropump in 1975. Their prototype was designed to be used as an implantable device in an artificial pancreas. The advent of microfabrication technologies and varied applications lent itself to the development of different types of micropumps. Micropumps have been classified based on working principle, driving mechanism, and chamber and valve design. Extensive reviews of micropumps and their classification have been presented by Laser and Santiago [4], Nguyen et al. [5], and more recently Woias [6].

Presented as Paper 0305 at the Aerospace Sciences, Reno, Nevada, 5–8 January 2004; received 29 March 2006; revision received 31 May 2007; accepted for publication 1 July 2007.

*Graduate Research Assistant, Center for Combustion and Environmental Research, Department of Mechanical Engineering.

†Professor, Center for Combustion and Environmental Research, Department of Mechanical Engineering, Associate Fellow AIAA.

‡Graduate Research Assistant, Center for Combustion and Environmental Research, Department of Mechanical Engineering; also Research Engineer, TDA Research Inc., 12345 West 52nd Avenue, Wheatridge, CO 80033, Member AIAA.

There have been numerous approaches to modeling micropumps. One dimensional [7], electrical analogy [8], lumped mass and lower-order models [9,10], and numerical techniques [9,11–13] are some of the methods that have been used to model micropumps. In the following, we first present simple analytical expressions to describe pump performance based mostly on the work of Olsson et al. [9]. We then carry out numerical analysis, first of the electrostatic force and resulting deflection of the diaphragm, and then of the resonant frequency of the diaphragm. We then analyze the steady behavior of the valves; lastly, we simulate the entire pump. In modeling the entire pump, we also address the large deformation effect of the membrane on pump performance.

The pump design we are working with consists of a chamber, an inlet and outlet valve, a flexible diaphragm, and an actuation mechanism as shown in Fig. 1. When the diaphragm is displaced upward, the chamber volume increases. The pressure within the chamber is less than the outside pressure. During this "supply" stroke, the inlet element acts as a diffuser and the outlet element as a nozzle, resulting in more fluid flowing in through the inlet than the outlet. As the diaphragm moves down, the chamber volume decreases. The pressure within the chamber is higher than the outside pressure, resulting in fluid flowing out through both the inlet and the outlet. However, due to the resistance characteristics of the elements, more fluid leaves the chamber through the outlet than the inlet. In this "pump" mode, the inlet element behaves like a nozzle and the outlet as a diffuser. In this way, over a complete cycle, fluid is pumped from the inlet to the outlet.

II. Analytical Relations Used to Assess Pump Characteristics

There are several issues relating to the characteristics of the pump, and it would be useful if the performance could be predicted using simple analytic relations, as numerical calculations are costly and complex.

The first is the driving mechanism. Electrostatic forces are used to drive the diaphragm. The driver is modeled as a parallel plate capacitor, with the diaphragm acting as a flexible electrode. The initial force between the pump diaphragm and the counter electrode is [14]

$$F = -\frac{\varepsilon_r \varepsilon_0 A V^2}{2g^2} \tag{1}$$

where ε_r is the relative permittivity of the dielectric medium, ε_0 is the permittivity of free space, A is the area of the electrodes, V is the potential difference between the electrodes, and g is the initial gap between the electrodes. As the diaphragm deforms, the gap between the electrodes decreases and as a consequence the force increases; in this way, the gap and force are coupled to each other. Another consequence of Eq. (1) is that the forcing function applied to the

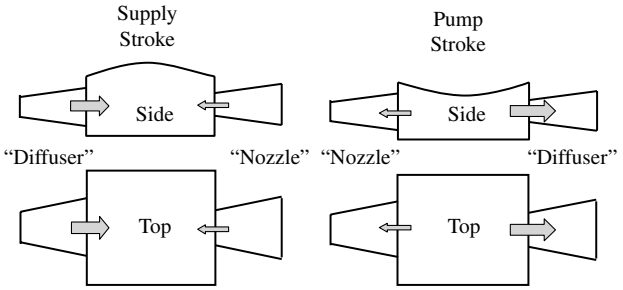

Fig. 1 Working principle of the micropump.

diaphragm is the square of the applied electrical forcing function, thus a sinusoidal voltage results in the diaphragm being forced with a sine squared function.

Linear theory [15] predicts that the centerline deflection of a square plate clamped on the four edges subject to a distributed static force is

$$y_0 = \frac{0.0138PL^4}{Eh^3} \tag{2}$$

where P is the distributed force, L the length of the side, E is the modulus of elasticity, and h is the thickness of the plate. Equation (2) is valid in the linear limit where deflection is less than about half the thickness and ignores the effect of stress stiffening. (Stress stiffening arises because the membrane is fixed on all sides. This causes the membrane to change stiffness with deflection.) In practice, both nonlinearity and stress stiffening may influence diaphragm behavior.

The natural frequency of the coupled diaphragm/fluid system can play an important role in determining the pump characteristics. Dynamic effects become significant when the operational frequency is close to the resonant frequency of the pump, or when the inertia of the fluid is important. In addition, several workers have noticed that the net flow rate through the pump tends to peak near the resonant frequency of the system. The resonant frequency of a square diaphragm clamped on the four edges, unaffected by the presence of fluid, is [16]

$$f = \frac{36h}{2\pi L^2}\sqrt{\frac{E}{12\rho(1-\nu^2)}} \tag{3}$$

where ν is Poisson's ratio, and ρ is the density of the diaphragm. The frequency of the first mode of the clamped diaphragm unaffected by the fluid was calculated to be 150 kHz. The response of the diaphragm is affected by the presence of fluid. The fluid acts like an added mass and reduces the resonant frequency of the membrane. For an inviscid, incompressible fluid, the fluid has the following effect [16]

$$\frac{f_{\text{fluid}}}{f_{\text{vacuum}}} = \left(1 + \frac{M_{\text{diaphragm}}}{M_{\text{fluid}}}\right)^{\frac{1}{2}} \tag{4}$$

where f_{fluid} and f_{vacuum} are the resonant frequencies of the diaphragm in the fluid and the vacuum, respectively, $M_{\text{diapgragm}}$ is the mass of the diaphragm, and M_{fluid} is the added mass of the fluid in contact with the diaphragm. For the pump, M_{fluid} is the entire mass of the fluid in the chamber. From Eq. (4), the effect of the fluid is shown to reduce the natural frequency by about 30% for the geometry and operating conditions explored next. However, the damped resonant frequency is far in excess of our operating frequencies, and so the dynamics of the diaphragm are essentially quasi static.

The diffuser/nozzle valve works on the principle of direction-dependent flow resistance. To provide flow rectification, the pressure drop in the diffuser direction must be less than that in the nozzle direction for the same flow rate. Following Olsson et al. [7], the net volumetric flow rate of the pump can be shown to be approximately

$$Q_{\text{net}} = 2V_0 f\left(\frac{\eta^{\frac{1}{2}} - 1}{\eta^{\frac{1}{2}} + 1}\right) \tag{5}$$

where V_0 is the displaced volume due to diaphragm motion, f is the operating frequency, and η is the valve effectiveness, defined as the ratio of nozzle to diffuser pressure loss coefficients

$$\eta = \frac{K_n}{K_d} \tag{6}$$

where K_n and K_d are the nozzle and diffuser loss coefficients, respectively.

Our analysis assumes that friction and pressure recovery dominate the pressure drop across the valve. (Calculation shows that entry and exit losses are negligible for the small Reynolds numbers encountered.) For simplicity, we use the average geometric properties of the valve to estimate frictional losses. Defining the average hydraulic diameter of the passage as

$$D_h = \frac{4A}{P} \tag{7}$$

where A and P are the average cross-sectional area and the wetted perimeter of the valve, respectively, the average Reynolds number is thus

$$Re = \frac{D_h U}{\nu} \tag{8}$$

where U is the average velocity and ν is the kinematic viscosity of the fluid. The Reynolds number is on the order of 10, thus the flow is laminar. The friction factor for laminar flow in a square duct can be approximated using the expression of Shah and London [17]

$$fRe = 24(1 - 1.3553\alpha + 1.9467\alpha^2 - 1.7012\alpha^3 + 0.9564\alpha^4 - 0.2537\alpha^5) \tag{9}$$

and the pressure loss due to friction is approximately that for steady-state constant area pipe flow

$$\Delta p_f = \frac{fL}{D_h}\rho\frac{U^2}{2} \tag{10}$$

where L is the length of the valve and ρ is the density of the fluid.

The frictionless pressure recovery due to an expansion is [18]

$$\Delta p_d = (1 - \text{AR}^2)\rho\frac{U^2}{2} \tag{11}$$

where AR is the area ratio of the valve.

Neglecting the entry and exit losses, because loss coefficients are small compared with the frictional term, assuming no flow separation and that pressure losses are due to friction and expansion/contraction only, the effectiveness of the valve becomes

$$\eta = \frac{\Delta p_{\text{nozzle}}}{\Delta p_{\text{diffuser}}} = \frac{\Delta p_f + \Delta p_d}{\Delta p_f - \Delta p_d} \tag{12}$$

III. Numerical Analysis

The ANSYS finite element analysis package was employed to conduct all the numerical simulations. ANSYS is a general purpose modeling package that may be used for structural, thermal, fluid, and electromagnetic analysis. Figure 2 shows a schematic of the pump with the dimensions that were used in both analytical and numerical calculations. The pump is fabricated from silicon with a nickel diaphragm.

A. Electrostatic-Structural Coupled Analysis

We conducted static electrostatic-structural coupled analysis to determine the voltage displacement relationship for the diaphragm

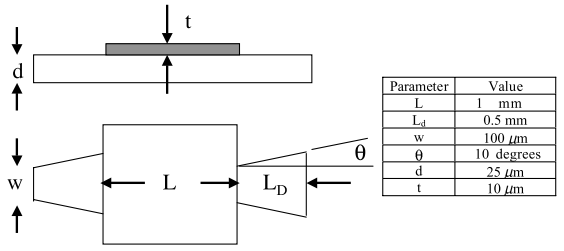

Parameter	Value
L	1 mm
L_d	0.5 mm
w	100 μm
θ	10 degrees
d	25 μm
t	10 μm

Fig. 2 Geometric parameters of the pump (*d* is the channel thickness).

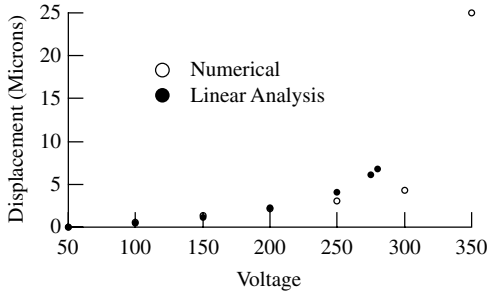

Fig. 3 Diaphragm displacement as a function of applied voltage.

and to explore the range of validity of the analytical expressions given by Eqs. (1) and (2). The coupled set of Eqs. (1) and (2) were solved to obtain the analytical results. The numerical solution was carried out using the electrostatic-structural solver in ANSYS. Figure 3 shows the displacement voltage relationship for both analytical and numerical calculations. We see that the analytical and numerical results are in close agreement below a voltage of about 250 V. Higher voltages leads to a deviation, with the analytical pull in voltage being lower than the numerically calculated value. The pull in voltage is the point at which the combination of nonlinear force increase and gap reduction results in a rapid increase in deflection. In microelectromechanical systems (MEMS) devices, the diaphragm may be deflected into contact with the opposing surface.

B. Analysis of the Valve Flow

To assess the validity of the simple valve analysis, a three-dimensional steady-state analysis of flow in the diffuser/nozzle valves was performed to determine the effect of velocity, valve depth, and valve half-angle on efficiency. Uniform pressure and velocity boundary conditions were imposed at the inlet and exit, respectively, with no slip boundary conditions used at the walls. The length of the diffuser was 0.5 mm, and the smaller width of the valve was 0.1 mm. A valve with a depth of 25 μm, a half-angle of 10 deg, and an inlet velocity of 0.1 m/s was considered as the base case. The depth, half-angle, and inlet velocity were then varied independently. The pressure drop across the valves in the diffuser and nozzle directions for a given flow rate was then calculated to find the effect of the preceding parameters on valve efficiency. Figures 4–6 show the results of the calculations. As seen in Fig. 4, the effectiveness of the valve increases approximately linearly with velocity. Because of low pump velocities, and consequently Reynolds number, the efficiency of the valves is very low. Figure 5 shows that an increase in depth increases the valve efficiency. The effect of half-angle is shown in Fig. 6, in which the effectiveness increases initially with half-angle and begins to level off. At higher Reynolds numbers, workers have shown that there exists a half-angle that maximizes the efficiency and is dependent on the Reynolds number and flow conditions [19]. It is obvious that the simplified analysis can be off by a considerable amount. This is not particularly surprising given the degree of approximations made. However, as discussed next, by calibrating the simple analysis by using numerical results, it can be useful.

C. Fluid-Structure Coupled Analysis of Complete Pump

We next conducted full pump simulations using the fluid-structure interaction (FSI) module in ANSYS. In the FSI macro, the fluid and

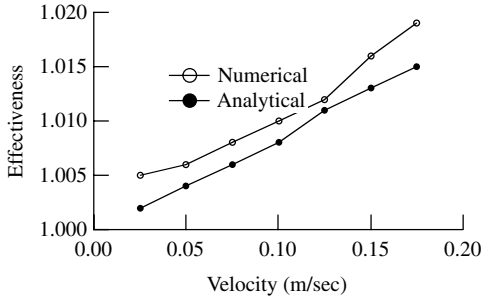

Fig. 4 Effect of velocity on nozzle effectiveness.

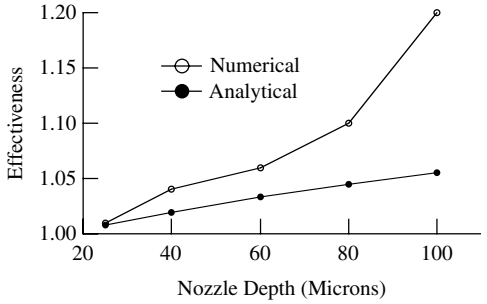

Fig. 5 Effect of nozzle/diffuser depth (constant velocity of 0.1 m/s) on effectiveness.

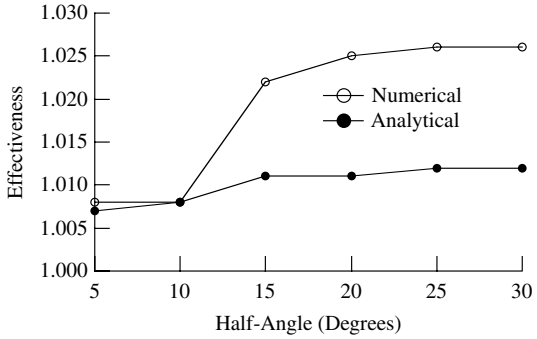

Fig. 6 Effect of nozzle/diffuser half-angle on effectiveness.

structural domains are sequentially solved with information exchanged at the fluid-structure interface to update the boundary conditions of both domains. Forces are transferred from the fluid to the structural domain, whereas displacements are transferred from the structural to the fluid domain at every time step. The arbitrary Lagrangian Eulerian (ALE) method is used to morph the fluid mesh to satisfy the boundary conditions as the diaphragm moves.

The following boundary conditions were used: a vertical plane of symmetry dividing the pump in half was used, the inlet and outlet were specified to be zero gauge pressure, and no slip conditions were applied at the walls. We assumed a sinusoidal electrical voltage input, which implies that the forcing pressure on the diaphragm varies with time as $\sin(t)^2$ if we ignore the effect of the changing gap. A linear solver was used for the first set of pump calculations with small membrane deflections, whereas the nonlinear solver was used for the second set of pump calculations so as to accurately model large deformations of the diaphragm. The nonlinear solver accounts for the changes in stiffness that occur due to changes in shape and orientation of the finite elements. All numerical calculations were considered mesh and time independent when a reduction in element size and time step produced little change in the solutions.

1. *Small Displacement Analysis*

The analysis was carried out on a pump with parameters as specified in Fig. 2. A pressure amplitude of 70 kPa was applied to the

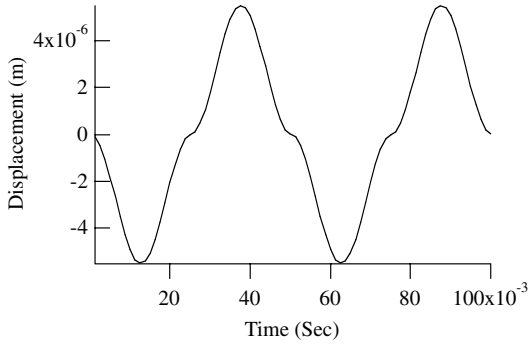

Fig. 7 Membrane displacement.

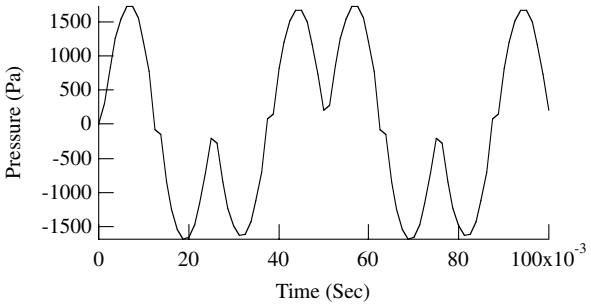

Fig. 8 Chamber pressure.

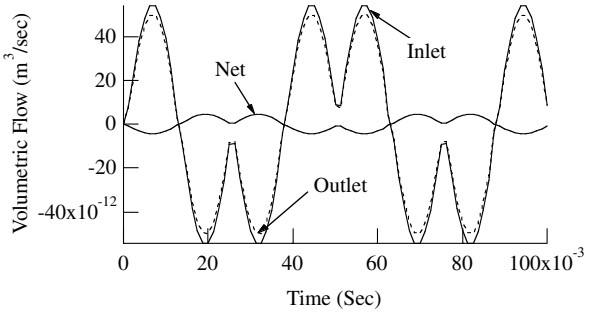

Fig. 9 Exit, inlet, and instantaneous flow rates.

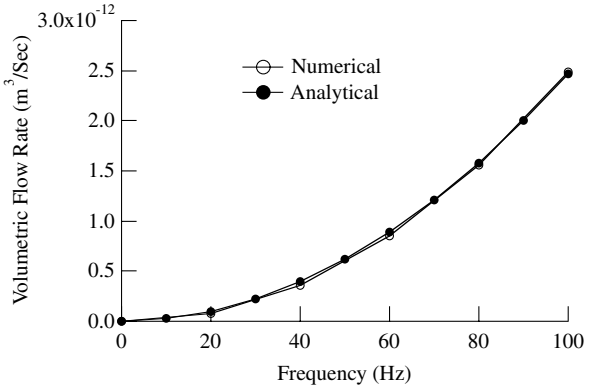

Fig. 10 The effect of actuation frequency on total net flow.

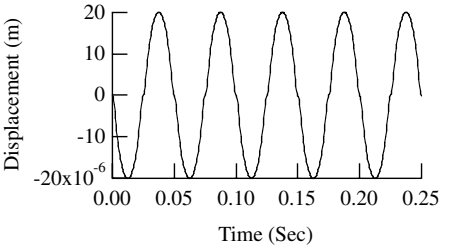

Fig. 11 Membrane displacement: nonlinear solver.

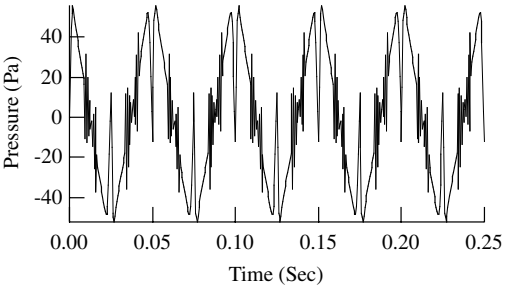

Fig. 12 Chamber pressure: nonlinear solver.

membrane, with the operating frequency varied from 0 to 100 Hz. Figure 7 shows the displacement of the membrane at its center at a frequency of 20 Hz. The membrane appears to follow the $\sin(t)^2$ forcing function. The maximum displacement is 5.5 μm. Figure 8 shows the pressure–time history for this case.

Figure 9 shows the exit, inlet, and net flow rate over two cycles. Because the valves are not perfect, the fluid flows both out of and into the inlet and outlet simultaneously during pump and supply strokes, respectively. The net flow rate is thus calculated as the difference between the exit and inlet flow rates. A positive net flow rate indicates a flow from the inlet to the outlet, which is the desired direction of pumping.

Figure 10 shows the numerical solution for the net flow rate for frequencies from 0 to 100 Hz, along with the analytic solution based on the discussion of Sec. II. The analytic solution will be discussed further in the next section.

2. Large Displacement Analysis

The large displacement analysis was conducted on a pump with the following changes: a chamber depth of 100 μm, a membrane of thickness of 10 μm, a valve of length 0.4 mm, a half-angle of 6^0, and an applied pressure amplitude of 10^6 Pa. The actuation frequency was varied from 0 to 100 Hz. The nonlinear structural solver was used.

Figure 11 shows the membrane displacement time history at an operating frequency of 20 Hz. The linear analytic expression predicts a displacement of $\sim$66 μm, whereas the numerical results predict about 20 μm. The difference can be attributed to stress stiffening. The pump chamber pressure is shown in Fig. 12. The oscillation in pressure arises from the nature of the forcing function and the nonlinear behavior of the membrane, and appears to be independent of time step.

The instantaneous flow rates are shown in Fig. 13. Figure 14 shows the net flow as a function of actuation frequency, along with the analytic solution based on the discussion of Sec. II. The analytic solution will be discussed further in the next section.

IV. Discussion

The numerical results demonstrate that a pump of the design considered here can operate in a positive flow mode, as has been demonstrated experimentally by Olsson et al. [7]. The passive valves are not particularly efficient at the low flow rates considered in our study, and numerical simulation must be used to optimize their design.

Not surprisingly, the simple analysis presented herein is not particularly accurate in the absolute sense, although it does capture the functional form of both valve efficiency and the volumetric flow rate–frequency relationship. To obtain the excellent agreement between the numerical and analytical results shown in Fig. 10, the average velocity used to calculate the valve efficiency was scaled to force agreement in Q_{net} at 100 Hz, and the maximum displacement of the diaphragm set to the numerical value. All other parameters were

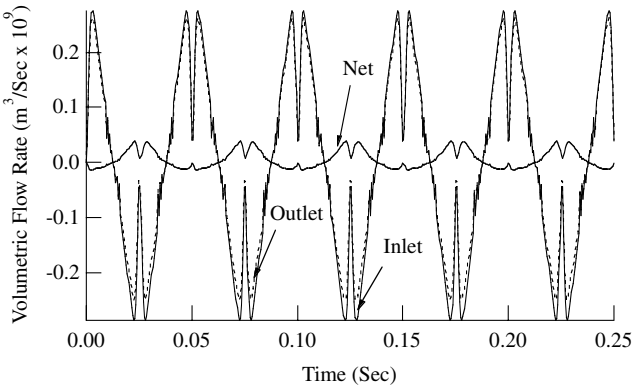

Fig. 13 Exit, inlet, and net instantaneous flows: nonlinear solver.

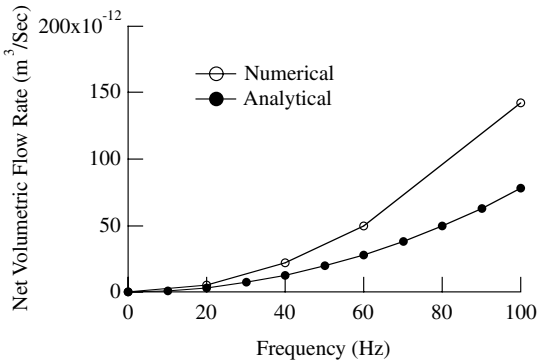

Fig. 14 The effect of actuation frequency on total net flow: nonlinear solver.

calculated directly from the geometry and fluid properties. For Fig. 14, the same scaling parameter for valve velocity was used as for Fig. 10, but with the maximum diaphragm displacement taken from the nonlinear solver result. The simple analysis thus underpredicts valve efficiency in this case and obtaining a better fit would require adjusting the scaling parameter.

The fluid mechanics of the valves are somewhat complex in actuality because the flow is unsteady and length scales are much smaller than historically explored. There are a number of conflicting models for valve efficiency in the literature, although with scaling they seem to perform at a level similar to ours. It does seem clear that macroscale results for loss coefficients of nozzles and valves operating at higher Reynolds numbers are not appropriate in our case, as they predict that losses for the nozzle direction are less than for the diffuser direction. This would result in net flow opposite to that observed. A clarification of this issue would be useful to the MEMS community, as valve design is the performance limiter for building practical pumps.

Although we did not numerically explore the sensitivity of our results to uncertainty in fabrication dimensions, one can do so using the analytic expressions. The volumetric flow rate [Eq. (5)] is directly proportional to the displaced volume and the operating frequency, and approximately proportional to the square root of the valve efficiency. How much each of these parameters varies in practice is, of course, device and fabrication-process dependent. Figures 5 and 6 may be used to assess the influence of geometry changes on the valve effectiveness for our design.

V. Conclusions

A detailed numerical analysis was carried out to calculate the characteristics of a micropump. Simple analytic expressions were presented to predict the diaphragm displacement, the valve efficiency, and the net flow rate through the pump. The linear analytic expression for diaphragm displacement as a result of electrostatic forcing is valid for small deflections; however, at higher voltages, this expression deviates from numerical results. The simple analytical model does properly mimic the functional form of both the valve efficiency and the net pump flow rate. However, it must be scaled to match the numerical results. Properly scaled, the simple analytical model can be used for design calculations.

Acknowledgment

Support from the U.S. Air Force Office of Scientific Research, Program Officer, Mitat Birkin, is gratefully acknowledged. Award no. F49620-02-1-0133.

References

[1] Brophy, C. M., Netzer, D. W., Sinibaldi, J., and Johnson, R., "Detonation of a JP-10 Aerosol for Pulse Detonation Engine Applications," *High-Speed Deflagration and Detonation: Fundamentals and Control*, ELEX KM Publishers, Moscow, 2000, pp. 207–221.

[2] Brophy, C. M., Sinibaldi, J. O., Netzer, D. W., and Johnson, R. G., "Operation of a JP-10/Air Pulse Detonation Engine," *36th AIAA/ASME/SAE/ASEE Joint Propulsion Conference*, AIAA Paper No. 2000-3591, 2000.

[3] Thomas, L. J., Jr., and Bessman, S. P., "Prototype for an Implantable Micropump Powered by Piezoelectric Disk Benders," *Transactions - American Society for Artificial Internal Organs*, Vol. 21, 1975, pp. 516–22.

[4] Laser, D. J., and Santiago, J. G., "A Review of Micropumps," *Journal of Micromechanics and Microengineering*, Vol. 14, No. 6, 2004, pp. R35–R64.
doi:10.1088/0960-1317/14/6/R01

[5] Nguyen, N. T., Huang, X., and Chuan, T. K., "MEMS-Micropumps: A Review," *Journal of Fluids Engineering*, Vol. 124, No. 2, 2002, pp. 384-392.
doi:10.1115/1.1459075

[6] Woias, P., "Micropumps: Past, Progress and Future Prospects," *Sensors and Actuators B, Chemical*, Vol. 105, No. 1, 2005, pp. 28–38.
doi:10.1016/S0925-4005(04)00108-X

[7] Olsson, A., Stemme, G., and Stemme, E., "A Valve-Less Planar Fluid Pump with Two Pump Chambers," *Sensors and Actuators A, Physical*, Vols. 47, Nos. 1–3, 1995, pp. 549–556.
doi:10.1016/0924-4247(94)00960-P

[8] Bourouina, T., and Grandchamp, J., "Modeling Micropump with Electrical Equivalent Networks," *Journal of Micromechanics and Microengineering*, Vol. 6, No. 4, 1996, pp. 398–404.
doi:10.1088/0960-1317/6/4/006

[9] Olsson, A., Stemme, G., and Stemme, E., "A Numerical Design Study of the Valveless Diffuser Pump Using a Lumped Mass Model," *Journal of Micromechanics and Microengineering*, Vol. 9, No. 1, 1999, pp. 34–44.
doi:10.1088/0960-1317/9/1/004

[10] Morris, C., and Foster, F., "Low-Order Modeling of Resonance for Fixed Valve Micropumps Based on First Principles," *Journal of Microelectromechanical Systems*, Vol. 12, No. 3, 2003, pp. 325–334.
doi:10.1109/JMEMS.2003.809965

[11] Pan, L., Ng, T., Wu, X., and Lee, H., "Analysis Of Valveless Micropumps with Inertial Effects," *Journal of Micromechanics and Microengineering*, Vol. 13, No. 3, 2003, pp. 390–399.
doi:10.1088/0960-1317/13/3/307

[12] Nguyen, N., and Huang, X., "Numerical Simulation of Pulse Width Modulated Micropumps with Diffuser/Nozzle Elements," *Technical Proceedings of the 2000 International Conference on Modeling and Simulation of Microsystems*, Nano Science and Technology Inst., Danville, CA, 2000, pp. 636–639.

[13] Fan, B., Song, G., and Hussain, F., " Simulation of a Piezoelectrically Actuated Valveless Micropump," *Smart Materials and Structures*, Vol. 14, No. 2, 2005, pp. 400–405.
doi:10.1088/0964-1726/14/2/014

[14] Senturia, S. D., *Microsystem Design*, Kluwer Academic, Norwell, MA, 2001.

[15] Roark, R. J., *Formulas for Stress and Strain*, 4th ed., McGraw–Hill, New York, 1964.

[16] Blevins, R. D., *Formulas for Natural Frequency and Mode Shape*, Krieger, Malabar, FL, 2001.

[17] Shah, R. K., and London, A. L., "Laminar Flow Forced Convection in Ducts," *Advances in Heat Transfer*, Vol. 1, Supplement 1, Academic Press, New York, 1978.

[18] Fox, R. W., McDonald, A. T., *Introduction to Fluid Mechanics*, 4th ed., Wiley, New York, 1992.

[19] Singhal, V., Garimella, S. V., and Murthy, J. Y., "Low Reynolds Number Flow Through Nozzle-Diffuser Elements in Valves Micropumps," *Sensors and Actuators A, Physical*, Vol. 113, No. 2, 2004, pp. 226–235.

doi:10.1016/j.sna.2004.03.002

J. Oefelein
Associate Editor